 

# Optically Active S-Bridged $Co^{III}M$ ($M = Pt^{II}$, $Hg^{II}$, $Au^{I}$) Polynuclear Complexes Derived from ΔΔ-$[Ni\{Co(aet)_2(R\text{-pn})\}_2]^{4+}$ (aet = 2-Aminoethanethiolate, *R*-pn = (*R*)-1,2-Propanediamine)

**Yasunori Yamada,* Yoshitaro Miyashita, Kiyoshi Fujisawa, and Ken-ichi Okamoto***

Department of Chemistry, University of Tsukuba, Tsukuba, Ibaraki 305-8571

(Received December 5, 2001)

The substitution reaction of ΔΔ-$[Ni\{Co(aet)_2(R\text{-pn})\}_2]^{4+}$ (aet = 2-aminoethanethiolate, *R*-pn = (*R*)-1,2- propanediamine) with an equimolar $K_2[PtCl_4]$ stereoselectively produced an optically active S-bridged trinuclear complex, ΔΔ-$[Pt\{Co(aet)_2(R\text{-pn})\}_2]^{4+}$ (**1**). A similar reaction with equimolar $Hg(ClO_4)_2\cdot 6H_2O$ also selectively gave the trinuclear complex, ΔΔ-$[Hg\{Co(aet)_2(R\text{-pn})\}_2]^{4+}$ (**2**). Contrary to **1** and **2**, a tetranuclear complex, ΔΔ-$[Au_2\{Co(aet)_2(R\text{-pn})\}_2]^{4+}$ (**3**), was obtained by a two-molar-equivalent addition of $[AuCl\{S(CH_2CH_2OH)_2\}]$. The crystal structures of **1**, **2**, and **3** were determined by X-ray crystallography. Each of the Co atoms in **1**, **2**, and **3** is coordinated by one *R*-pn and two aet ligands to form an octahedron with a Δ configuration. The Pt atom in **1** is coordinated by four S atoms from two Δ-*cis*(*S*)-$[Co(aet)_2(R\text{-pn})]^+$ units to take a square-planar geometry. Although the Hg atom in **2** is also surrounded by four S atoms from two Δ-*cis*(*S*)-$[Co(aet)_2(R\text{-pn})]^+$ units, the geometry around the Hg center is of an appreciably distorted tetrahedron. On the other hand, each of the two Au atoms is bridged by an S atom from one *cis*(*S*)-$[Co(aet)_2(R\text{-pn})]^+$ unit and an S atom from another unit to form a $Co_2Au_2S_4$ eight-membered ring. These complexes are characterized based on the electronic absorption, CD, and $^{13}C$ NMR spectra.

The chemistry for the S-bridged polynuclear complexes has been partly developed based on the S-donating abilities of mononuclear complexes ligated by 2-aminoethanethiolate (aet) and the related compounds. A wide variety of metal ions and complexes can be actually incorporated into S-bridged polynuclear structures with the aid of such S-donating metalloligands.[1–15] Although the diversity in both the structural and physicochemical properties are generated for these S-bridged polynuclear complexes, their structural motifs are mainly governed by only two factors, i.e., the coordination modes of incorporated metal ions and the geometries of metalloligands.[4–15] Accordingly, alternative use of the metalloligands and incorporated metals is expected to make regulation of the polynuclear structures possible. Regarding metalloligands with octahedral geometries, however, the possibility for a pair of enantiomers with the Δ and Λ configurations complicates the stereochemistry for the polynuclear structures.[4] For the purpose of simplifications concerning the stereochemical characters of S-bridged polynuclear complexes composed of octahedral units, the metalloligands involving optically active ligands seem to be of a great advantage for the preclusion of enantiomeric intricacy. Recently, we have shown that an optically active S-bridged trinuclear complex, ΔΔ-$[Ni\{Co(aet)_2(R\text{-pn})\}_2]^{4+}$ (*R*-pn = (*R*)-1,2-propanediamine), is stereoselectively obtained by the reaction of $[Ni(aet)_2]$ with $[CoCl_2(R\text{-pn})_2]^+$.[16] Furthermore, it was found more recently that the central $Ni^{2+}$ ion in ΔΔ-$[Ni\{Co(aet)_2(R\text{-pn})\}_2]^{4+}$ is readily substituted by the $Pd^{2+}$ ion, or its complexes, while retaining the absolute configurations of the octahedral Co(III) units.[17] These facts indicate that the Δ-*cis*(*S*)-$[Co(aet)_2(R\text{-pn})]^+$ units in the complex can be regarded as an optically active metalloligand with two donating S-atoms. It is therefore expected that the stereoselective construction of a wide variety of optically active S-bridged polynuclear complexes including Δ-*cis*(*S*)-$[Co(aet)_2(R\text{-pn})]^+$ units are made possible by applying substitution reactions of ΔΔ-$[Ni\{Co(aet)_2(R\text{-pn})\}_2]^{4+}$ with metal ions. In addition, the use of ΔΔ-$[Ni\{Co(aet)_2(R\text{-pn})\}_2]^{4+}$ provides information about the aggregation of optically active S-donating metalloligands around various metal centers. In the present paper, we report on the syntheses, crystal structures and spectrochemical characterizations of the S-bridged $Co^{III}M$ ($M = Pt^{II}$, $Hg^{II}$, $Au^{I}$) polynuclear complexes, ΔΔ-$[Pt\{Co(aet)_2(R\text{-pn})\}_2]^{4+}$ (**1**), ΔΔ-$[Hg\{Co(aet)_2(R\text{-pn})\}_2]^{4+}$ (**2**), and ΔΔ-$[Au_2\{Co(aet)_2(R\text{-pn})\}_2]^{4+}$ (**3**), which were stereoselectively derived from substitution reactions of ΔΔ-$[Ni\{Co(aet)_2(R\text{-pn})\}_2]^{4+}$.

## Experimental

**Materials.** 2,2′-Thiodiethanol, sodium hexafluorophosphate and potassium tetrachloroplatinate(II) were purchased from Tokyo Chemical Co., Ltd., Aldrich Chemical Co., Inc., and Tanaka Rare Metal Industries Ltd., respectively. Mercury(II) perchlorate hexahydrate, sodium tetrachloroaurate(III) dihydrate, and sodium perchlorate hexahydrate were obtained from Wako Pure Chemical Ind. Co., Ltd., and the other chemicals from Wako Pure Chemical Ind. Co., Ltd., or Tokyo Chemical Co., Ltd. All of the chemicals were of reagent grade and used without further purification. The starting complex, ΔΔ-$[Ni\{Co(aet)_2(R\text{-pn})\}_2](ClO_4)_4\cdot H_2O$, for the present polynuclear complexes was prepared by a previously reported procedure.[16]

**Preparation of Complexes. ΔΔ-$[Pt\{Co(aet)_2(R\text{-pn})\}_2]^{4+}$ (1).** To a solution containing 0.26 g (0.25 mmol) of ΔΔ-$[Ni\{Co(aet)_2$-

($R$-pn)}$_2$]$(ClO_4)_4$·$H_2O$ in 50 cm$^3$ of water was added a solution containing 0.10 g (0.25 mmol) of $K_2[PtCl_4]$ in 10 cm$^3$ of water. After the mixture was stirred at 55°C for 1 h, 10 cm$^3$ of a saturated $NaPF_6$ solution was added to the resulting dark-red solution. The whole was allowed to stand at room temperature for several days, and the resulting dark-red crystals were collected by filtration. A well-formed crystal of **1**$(PF_6)_4$·$2H_2O$ was used for an X-ray structural analysis. It was confirmed by SP-Sephadex C-25 column chromatography using a solution of $[Sb_2(d\text{-tartrato})_2]^{2-}$ as an eluent that all of the crystals contain only the optically active isomer with Δ-*cis*(*S*)-[Co(aet)$_2$(*R*-pn)]$^+$ units to show a negative CD sign around 500 nm in solution. Yield: 0.29 g (84%). Calcd for [Pt{Co(aet)$_2$(*R*-pn)}$_2$]$(PF_6)_4$·$2H_2O$ = $C_{14}H_{48}N_8O_2F_{24}P_4S_4Co_2Pt$: C, 12.17; H, 3.49; N, 8.11%. Found: C, 12.20; H, 3.52; N, 8.07%.

**ΔΔ-[Hg{Co(aet)$_2$(*R*-pn)}$_2$]$^{4+}$ (2).** To a solution containing 0.26 g (0.25 mmol) of ΔΔ-[Ni{Co(aet)$_2$(*R*-pn)}$_2$]$(ClO_4)_4$·$H_2O$ in 50 cm$^3$ of acetonitrile was added 0.20 g (0.25 mmol) of Hg$(ClO_4)_2$·$6H_2O$ in 10 cm$^3$ of acetonitrile. After the mixture was stirred at 55°C for 1 h, 10 cm$^3$ of a saturated $NaClO_4$ aqueous solution was added to the resulting dark-red acetonitrile solution. The whole was allowed to stand at room temperature for several days, and the resulting dark-red crystals were collected by filtration. A well-formed crystal of **2**$(ClO_4)_4$·$9H_2O$ was used for an X-ray structural analysis. It was confirmed by the SP-Sephadex C-25 column chromatography using a solution of $[Sb_2(d\text{-tartrato})_2]^{2-}$ as an eluent that all of the crystals contain only the optically active isomer with Δ-*cis*(*S*)-[Co(aet)$_2$(*R*-pn)]$^+$ units to show a negative CD sign around 500 nm in solution. Yield: 0.23 g (70%). Calcd for [Hg{Co(aet)$_2$(*R*-pn)}$_2$]$(ClO_4)_4$·$9H_2O$ = $C_{14}H_{62}N_8O_{25}S_4Cl_4Co_2Hg$: C, 12.63; H, 4.69; N, 8.42%. Found: C, 12.61; H, 4.70; N, 8.38%.

**ΔΔ-[Au$_2${Co(aet)$_2$(*R*-pn)}$_2$]$^{4+}$ (3).** To a solution containing 0.20 g (0.50 mmol) of Na[$AuCl_4$]·$2H_2O$ in 4 cm$^3$ of water was added 0.32 cm$^3$ of 2,2′-thiodiethanol for the preparation of a solution of [AuCl{$S(CH_2CH_2OH)_2$}] involving the Au(I) species. The resulting colorless solution was added to a solution containing 0.26 g (0.25 mmol) of ΔΔ-[Ni{Co(aet)$_2$(*R*-pn)}$_2$]$(ClO_4)_4$·$H_2O$ in 50 cm$^3$ of water. After the mixture was stirred at 55°C for 1 h, 10 cm$^3$ of a saturated $NaClO_4$ solution was added to the resulting dark-red solution. The whole was allowed to stand at room temperature for several days, and the resulting dark-red crystals were collected by filtration. A well-formed crystal of **3**$(ClO_4)_4$·$H_2O$ was used for an X-ray structural analysis. It was confirmed by the SP-Sephadex C-25 column chromatography using a solution of $[Sb_2(d\text{-tartrato})_2]^{2-}$ as an eluent that all of the crystals contain only the optically active isomer with Δ-*cis*(*S*)-[Co(aet)$_2$(*R*-pn)]$^+$ units to show negative CD sign around 500 nm in solution. Yield: 0.26 g (76%). Calcd for [Au$_2${Co(aet)$_2$(*R*-pn)}]$(ClO_4)_4$·$H_2O$ = $C_{14}H_{46}N_8O_{17}S_4Cl_4Co_2Au_2$: C, 12.18; H, 3.36; N, 8.12%. Found: C, 12.19; H, 3.41; N, 8.07%.

**Measurements.** The electronic absorption spectra were recorded with a JASCO Ubest V-560 spectrophotometer, and the CD spectra with a JASCO J-600 spectropolarimeter. All of the measurements were carried out in aqueous solutions at room temperature. The $^{13}C$ NMR spectra were recorded with a Bruker AVANCE-600 NMR spectrometer in a 1:1 mixed solvent of $CD_3CN$ and $D_2O$, using tetramethylsilane (TMS) as an internal reference. The elemental analyses (C, H, N) were performed by the Analysis Center of the University of Tsukuba.

**Crystallography.** The unit-cell parameters and intensity data for **1**$(PF_6)_4$·$2H_2O$, **2**$(ClO_4)_4$·$9H_2O$, and **3**$(ClO_4)_4$·$H_2O$ were used for data collection on a Rigaku RASA-7S four-circle diffractometer with graphite-monochromatized Mo$K\alpha$ radiation. The unit-cell parameters were determined by a least-square refinement of 25 reflections for **1**$(PF_6)_4$·$2H_2O$ and **2**$(ClO_4)_4$·$9H_2O$, and 24 reflections for **3**$(ClO_4)_4$·$H_2O$ ($11° < \theta < 14°$). The crystal data and experimental parameters are listed in Table 1. The intensity data were collected by the $\omega$–$2\theta$ scan technique, and the intensities were corrected for Lorentz and polarization. An empirical absorption correction based on a series of $\Psi$ scans was applied. Indepen-

Table 1. Crystallographic Data of ΔΔ-[Pt{Co(aet)$_2$(*R*-pn)}$_2$]$(PF_6)_4$·$2H_2O$ (**1**$(PF_6)_4$·$2H_2O$), ΔΔ-[Hg{Co(aet)$_2$(*R*-pn)}$_2$]-$(ClO_4)_4$·$9H_2O$ (**2**$(ClO_4)_4$·$9H_2O$), and ΔΔ-[Au$_2${Co(aet)$_2$(*R*-pn)}$_2$]$(ClO_4)_4$·$H_2O$ (**3**$(ClO_4)_4$·$H_2O$)

| | **1**$(PF_6)_4$·$2H_2O$ | **2**$(ClO_4)_4$·$9H_2O$ | **3**$(ClO_4)_4$·$H_2O$ |
|---|---|---|---|
| Formula | $C_{14}H_{48}N_8O_2F_{24}P_4S_4Co_2Pt$ | $C_{14}H_{62}N_8O_{25}S_4Cl_4Co_2Hg$ | $C_{14}H_{46}N_8O_{17}S_4Cl_4Co_2Au_2$ |
| Fw | 1381.64 | 1331.20 | 1380.41 |
| Cryst dimens / mm | 0.30 × 0.34 × 0.18 | 0.40 × 0.40 × 0.25 | 0.10 × 0.20 × 0.25 |
| Space group | $P4_32_12$ | $I222$ | $P2_1$ |
| $a$ / Å | 13.253(2) | 14.462(6) | 12.947(3) |
| b / Å | | 20.640(5) | 16.68(2) |
| c / Å | 23.945(4) | 9.033(2) | 9.321(2) |
| $\beta$ / deg | | | 101.00(1) |
| $V$ / Å$^3$ | 4205(1) | 2696(1) | 1976(1) |
| $Z$ | 4 | 2 | 2 |
| $D_{calcd}$ / g cm$^{-3}$ | 2.182 | 1.639 | 2.320 |
| $\mu$ / cm$^{-1}$ | 45.74 | 38.81 | 88.06 |
| Transm factor | 0.81 – 1.00 | 0.52 – 1.00 | 0.59 – 1.00 |
| Scan type | $\omega$–$2\theta$ | $\omega$–$2\theta$ | $\omega$–$2\theta$ |
| $2\theta$ range / deg | 55.0 | 55.0 | 55.2 |
| No. of reflcns measd | 3013 | 1833 | 5058 |
| No. of reflcns used | 2127 | 1374 | 3230 |
| No. of variables used | 269 | 141 | 380 |
| $R$ ($R_w$) | 0.045( 0.054) | 0.039(0.056) | 0.043(0.056) |
| GOF | 1.14 | 1.49 | 1.24 |
| Flack parameter | −0.02(2) | −0.07(1) | −0.03(2) |

dent reflections with $I_0 > 2\sigma(I_0)$ were used for structure determinations. The positions of the Co, Pt, Au, Hg, and other non-H atoms were determined by a direct method. Difference Fourier maps based on these atomic positions revealed some remaining non-hydrogen atoms. The structures were refined by a full-matrix least-squares refinement on F of the positional parameters and the anisotropic thermal parameters of the non-hydrogen atoms, except for O atoms of the perchlorate anions in **3**$(ClO_4)_4 \cdot H_2O$, which were refined isotropically. The hydrogen atoms on the ligands were fixed by the geometrical and thermal constraints (C–H = N–H = 0.95 Å and $U = 1.3U$ (C, N)). For $(-)^{CD}{}_{500}$-**1**$(PF_6)_4 \cdot 2H_2O$, $(-)^{CD}{}_{500}$-**2**$(ClO_4)_4 \cdot 9H_2O$, and $(-)^{CD}{}_{500}$-**3**$(ClO_4)_4 \cdot H_2O$, when the refinements were carried out using sets of parameters containing the Δ configurations of the *cis*(*S*)-[Co(aet)$_2$(*R*-pn)]$^+$ units, the Flack parameters gave the values of −0.02(2) for **1**$(PF_6)_4 \cdot 2H_2O$, −0.07(1) for **2**$(ClO_4)_4 \cdot 9H_2O$, and −0.03(2) for **3**$(ClO_4)_4 \cdot H_2O$.[18,19] Furthermore, each of the asymmetric carbon atoms of the 1,2-propanediamine ligands in the Δ configurations shows the *R* configuration, which is expected for the used ligand. It can therefore be assumed that all of the *cis*(*S*)-[Co(aet)$_2$(*R*-pn)]$^+$ units in $(-)^{CD}{}_{500}$ complex cations take the Δ configuration. All of the calculations were performed on Indigo II computer using teXsan.[20] The final atomic positional parameters are deposited in Tables S1 – S9.[21] Crystallographic data have been deposited at the CCDC, 12 Union Road, Cambridge CB2 1EZ, UK and copies can be obtained on request, free of charge, by quoting the publication citation and the deposition numbers 178537–178539.

## Results and Discussion

**Syntheses.** The substitution reaction of ΔΔ-[Ni{Co(aet)$_2$(*R*-pn)}$_2$]$^{4+}$ with an equimolar $K_2[PtCl_4]$ stereoselectively produced an S-bridged trinuclear complex, ΔΔ-[Pt{Co(aet)$_2$(*R*-pn)}$_2$]$^{4+}$ (**1**). A similar reaction of ΔΔ-[Ni{Co(aet)$_2$(*R*-pn)}$_2$]$^{4+}$ with an equimolar amount of $Hg(ClO_4)_2 \cdot 6H_2O$ gave an S-bridged trinuclear complex, ΔΔ-[Hg{Co(aet)$_2$(*R*-pn)}$_2$]$^{4+}$ (**2**). In addition, the reaction of ΔΔ-[Ni{Co(aet)$_2$(*R*-pn)}$_2$]$^{4+}$ with two molar equivalent amounts of [AuCl{S($CH_2CH_2OH$)$_2$}] resulted in the formation of an S-bridged tetranuclear complex, ΔΔ-[Au$_2${Co(aet)$_2$(*R*-pn)}$_2$]$^{4+}$ (**3**). These facts indicate that the central $Ni^{2+}$ ion in ΔΔ-[Ni{Co(aet)$_2$(*R*-pn)}$_2$]$^{4+}$ is readily replaced by the $Pt^{2+}$, $Hg^{2+}$, or $Au^+$ ion. Furthermore, the $Pt^{2+}$ ion in **1**, the $Hg^{2+}$ ion in **2**, and the $Au^+$ ions in **3** were not replaced by the $Ni^{2+}$ ions, even when **1**, **2**, and **3** were treated with an excess amount of $Ni(ClO_4)_2 \cdot 6H_2O$. It therefore seems that the Pt–S bonds in **1**, the Hg-S bonds in **2**, and the Au–S bonds in **3** are considerably stronger than the Ni–S bonds in ΔΔ-[Ni{Co(aet)$_2$(*R*-pn)}$_2$]$^{4+}$. All of the octahedral *cis*(*S*)-[Co(aet)$_2$(*R*-pn)]$^+$ units in these complexes take Δ configurations, as expected from the fact that the starting complex, [Ni{Co(aet)$_2$(*R*-pn)}$_2$]$^{4+}$, is of the ΔΔ configuration.[16] Additionally, the substitution reaction of ΔΔ-[Ni{Co(aet)$_2$(*R*-pn)}$_2$]$^{4+}$ with the $Pd^{2+}$ ion or its complexes gave the S-bridged Co(III)–Pd(II) polynuclear complexes, during which the octahedral Δ-*cis*(*S*)-[Co(aet)$_2$(*R*-pn)]$^+$ units retain their absolute configurations.[17] It can therefore be concluded that the Δ-*cis*(*S*)-[Co(aet)$_2$(*R*-pn)]$^+$ units in ΔΔ-[Ni{Co(aet)$_2$(*R*-pn)}$_2$]$^{4+}$ can be regarded as an optically active metalloligand with two donating S-atoms.

**Crystal Structures.** An X-ray structural analysis for **1**$(PF_6)_4 \cdot 2H_2O$ revealed the presence of a discrete tetravalent complex cation, four hexafluorophosphate anions, and two $H_2O$ molecules. In the complex cation **1**, the central Pt atom is surrounded by four S atoms from two *cis*(*S*)-[Co(aet)$_2$(*R*-pn)]$^+$ units to form a trinuclear structure (Fig. 1). The overall structure of **1** is almost identical to those of [Ni{Co(aet)$_2$(*R*-pn)}$_2$]$^{4+}$ and [Pd{Co(aet)$_2$(*R*-pn)}$_2$]$^{4+}$,[16,17] except for differences of the central metal ions. In fact, the bond distances and angles in the two terminal Co(III) units are almost the same as those observed for [Ni{Co(aet)$_2$(*R*-pn)}$_2$]$^{4+}$ and [Pd{Co(aet)$_2$(*R*-pn)}$_2$]$^{4+}$ (Table 2). These imply that only the central $Ni^{2+}$ ion in the starting material is replaced by the $Pt^{2+}$ ion. The $CoN_2S_2$ equatorial plane and the $PtS_4$ plane in **1** are essentially coplanar (dihedral angles; av 7.9°), as in the cases of [Ni{Co(aet)$_2$(*R*-pn)}$_2$]$^{4+}$ (av 11.1°) and [Pd{Co(aet)$_2$(*R*-pn)}$_2$]$^{4+}$ (av 12.2°). On the other hand, the central $PtS_4$ sphere in **1** is slightly distorted from a square-planar to a tetrahedral geometry, in which the $PtS_1S_2$ and $PtS_1{}^*S_2{}^*$ planes intersect to form a dihedral angel of 9.3°, but the extent of the distortion is considerably smaller than those of the $NiS_4$ sphere in [Ni{Co(aet)$_2$(*R*-pn)}$_2$]$^{4+}$ (13.9°) and $PdS_4$ sphere in [Pd{Co(aet)$_2$(*R*-pn)}$_2$]$^{4+}$ (12.4°). This indicates that the Pt(II) atom in **1** is more liable to take a square-planar geometry than the Ni(II) atom in [Ni{Co(aet)$_2$(*R*-pn)}$_2$]$^{4+}$ and the Pd(II) atom in [Pd{Co(aet)$_2$(*R*-pn)}$_2$]$^{4+}$. The Pt–S distances (av 2.316(3) Å) in **1** are significantly longer than the Ni–S distances (av 2.206(5) Å) in [Ni{Co(aet)$_2$(*R*-pn)}$_2$]$^{4+}$, but are approximately equivalent to

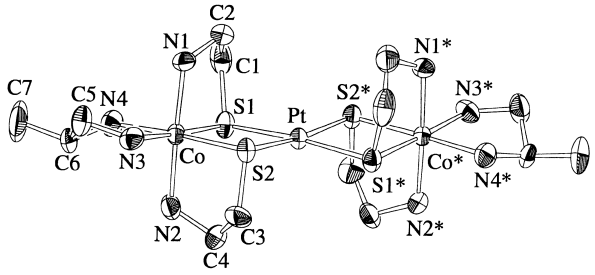


Fig. 1. Perspective view of ΔΔ-[Pt{Co(aet)$_2$(*R*-pn)}$_2$]$^{4+}$ (**1**) with the atomic labeling scheme.

Table 2. Selected Bond Distances (Å) and Angles (deg) of ΔΔ-[Pt{Co(aet)$_2$(*R*-pn)}$_2$](PF$_6$)$_4$·2H$_2$O (**1**(PF$_6$)$_4$·2H$_2$O)

| | | | |
|---|---|---|---|
| Pt–S(1) | 2.312(3) | Pt–S(1)* | 2.312(3) |
| Pt–S(2) | 2.319(3) | Pt–S(2)* | 2.319(3) |
| Co–S(1) | 2.239(3) | Co–S(2) | 2.253(3) |
| Co–N(1) | 1.978(9) | Co–N(2) | 1.973(10) |
| Co–N(3) | 1.988(10) | Co–N(4) | 1.997(9) |
| | | | |
| S(1)–Pt–S(1)* | 174.7(2) | S(1)–Pt–S(2) | 83.61(9) |
| S(1)–Pt–S(2)* | 96.71(9) | S(1)*–Pt–S(2) | 96.71(9) |
| S(1)*–Pt–S(2)* | 83.61(9) | S(2)–Pt–S(2)* | 173.0(2) |
| S(1)–Co–S(2) | 86.8(1) | S(1)–Co–N(1) | 88.0(3) |
| S(1)–Co–N(2) | 91.0(3) | S(1)–Co–N(3) | 177.2(3) |
| S(1)–Co–N(4) | 94.8(3) | S(2)–Co–N(1) | 90.6(3) |
| S(2)–Co–N(2) | 87.1(3) | S(2)–Co–N(3) | 93.9(3) |
| S(2)–Co–N(4) | 177.0(3) | N(1)–Co–N(2) | 177.5(4) |
| N(1)–Co–N(3) | 89.2(4) | N(1)–Co–N(4) | 92.0(4) |
| N(2)–Co–N(3) | 91.8(4) | N(2)–Co–N(4) | 90.3(4) |
| N(3)–Co–N(4) | 84.6(4) | Pt–S(1)–Co | 95.02(10) |
| Pt–S(2)–Co | 94.48(10) | | |

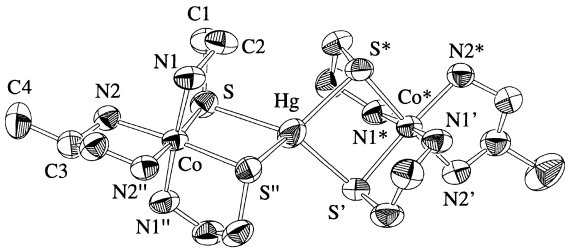


Fig. 2. Perspective view of ΔΔ-[Hg{Co(aet)$_2$(*R*-pn)}$_2$]$^{4+}$ (**2**) with the atomic labeling scheme.

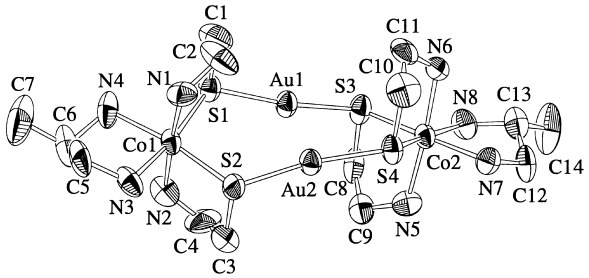


Fig. 3. Perspective view of ΔΔ-[Au$_2${Co(aet)$_2$(*R*-pn)}$_2$]$^{4+}$ (**3**) with the atomic labeling scheme.

Table 3. Selected Bond Distances (Å) and Angles (deg) of ΔΔ-[Hg{Co(aet)$_2$(*R*-pn)}$_2$](ClO$_4$)$_4$·9H$_2$O (**2**(ClO$_4$)$_4$·9H$_2$O)

| | | | |
|---|---|---|---|
| Hg–S | 2.562(2) | Hg–S″ | 2.562(2) |
| Hg–S* | 2.562(2) | Hg–S′ | 2.562(2) |
| Co–S | 2.246(2) | Co–S″ | 2.246(2) |
| Co–N(1) | 1.958(6) | Co–N(1)″ | 1.958(6) |
| Co–N(2) | 1.983(6) | Co–N(2)″ | 1.983(6) |
| | | | |
| S–Hg–S″ | 79.76(8) | S–Hg–S* | 115.54(8) |
| S–Hg–S′ | 138.30(9) | S″–Hg–S* | 138.30(9) |
| S″–Hg–S′ | 115.54(8) | S*–Hg–S′ | 79.76(8) |
| S–Co–S″ | 94.02(10) | S–Co–N(1) | 87.8(2) |
| S–Co–N(1)″ | 89.9(2) | S–Co–N(2) | 90.5(2) |
| S–Co–N(2)″ | 175.2(2) | S″–Co–N(1) | 89.9(2) |
| S″–Co–N(1)″ | 87.8(2) | S″–Co–N(2) | 175.2(2) |
| S″–Co–N(2)″ | 90.5(2) | N(1)–Co–N(1)″ | 176.6(4) |
| N(1)–Co–N(2) | 91.9(3) | N(1)–Co–N(2)″ | 90.6(3) |
| N(1)″–Co–N(2) | 90.6(3) | N(1)″–Co–N(2)″ | 91.9(3) |
| N(2)–Co–N(2)″ | 85.1(4) | Hg–S–Co | 93.11(6) |

the Pd–S distances (av 2.321(5) Å) in [Pd{Co(aet)$_2$(*R*-pn)}$_2$]$^{4+}$. Considering the covalent radii of the Ni, Pd and Pt metals, it would be expected that the Pt–S distances in **1** are longer than either the Ni–S ones in [Ni{Co(aet)$_2$(*R*-pn)}$_2$]$^{4+}$ or the Pd–S distancese in [Pd{Co(aet)$_2$(*R*-pn)}$_2$]$^{4+}$. Therefore, the identical distances of the Pt–S bonds in **1** with the Pd–S bonds in [Pd{Co(aet)$_2$(*R*-pn)}$_2$]$^{4+}$ seems to be interpreted as an effect of the lanthanide contraction for the Pt atom and/or a result of the stronger affinity with the S atoms of the Pt atom than that of the Pd atom.

As shown in Fig. 2, the complex cation **2** consists of two *cis*(*S*)-[Co(aet)$_2$(*R*-pn)]$^+$ units and one Hg atom, and behaves a different type of S-bridged trinuclear structure from **1** incorporated with a square-planar metal ion. The central Hg atom is coordinated by four S atoms from two Co(III) units to build up a distorted HgS$_4$ tetrahedron, in which the HgSS″ and HgS*S′ planes intersect to form a dihedral angel of 67.4°. However, the Hg–S distance (2.562(2) Å) in **2** is almost identical to those found in tetrahedral [Hg(thiolato-*S*)$_4$]$^{2-}$ (Table 3).[22,23] Since no counter anions and solvent molecules are in a close proximity to the Hg(II) center, the distortion may be attributed to a cross-plane interaction between the aet chelate rings of the two *cis*(*S*)-[Co(aet)$_2$(*R*-pn)]$^+$ units. The Hg–S–Co bridging angles (av 93.11(6)°) are slightly different from the corresponding angles in the trinuclear complexes with square-planar d$^8$ metal ions, such as Ni(II), Pd(II), and Pt(II).[16,17] Furthermore, the bond distances and angles around the two terminal Co(III) units, especially for the CoS$_2$N$_2$ equatorial planes, are considerably distinct from [Ni{Co(aet)$_2$(*R*-pn)}$_2$]$^{4+}$, [Pd{Co(aet)$_2$(*R*-pn)}$_2$]$^{4+}$, and **1**. For instance, the S–Co–S bite angle in **2** (94.02(10)°) is significantly obtuse compared with those in [Ni{Co(aet)$_2$(*R*-pn)}$_2$]$^{4+}$ (av 85.5(2)°), [Pd{Co(aet)$_2$(*R*-pn)}$_2$]$^{4+}$ (av 88.2(2)°), and **1** (86.8(1)°). These are reflected by the geometrical differences of the metal ions incorporated into the S-bridged trinuclear structures.

Contrary to the trinuclear structures of **1** and **2**, complex cation **3** contains two Co and two Au atoms to form a tetranuclear structure (Fig. 3). Each of the two Au atoms is bridged by one S atom from one *cis*(*S*)-[Co(aet)$_2$(*R*-pn)]$^+$ unit and one S atom from another unit. The distinctions from **1** and **2** are found in the bond distances and angles with respect to the two terminal *cis*(*S*)-[Co(aet)$_2$(*R*-pn)]$^+$ units, reflecting the coordination numbers of the incorporated metal ions (Table 4). For instance, the Au–S–Co bridging angles (av 118.6(2)°) are significantly different from those of Pt–S–Co (av 94.75(10)°) in **1** and those of Hg–S–Co (av 93.11(6)°) in **2**. As a result, the terminal Co(III) units are forced to the distorted octahedron compared with those in **1** and **2**. For instance, the S–Co–S bite angles in **3** (av 102.02(10)°) are significantly deviated from the ideal value of 90° for the octahedron, and are obtuse compared with those in **1** (86.8(1)°) and **2** (94.02(10)°). It is noteworthy that the S–Au–S linkages are highly deviated from linearity with angles of av 167.5(1)°, and that the two Au atoms are situated in the vicinity of each other with a Au1–Au2 distance of 2.8775(7) Å, which is within the range of the Au–Au contact.[23–25] Since the distances and angles around the Au1 center are almost the same as those around the Au2 center, it can be regarded that the two Au atoms in the complex are almost equivalent to each other.

All of the complexes with *R*-pn ligands selectively gave only optically active isomers. Taking the absolute configurations (Δ and Λ) of the *cis*(*S*)-[Co(aet)$_2$(*R*-pn)]$^+$ units into consideration, three isomers (ΔΔ, ΛΛ, and ΔΛ) are possible for **1**, **2**, and **3**. X-ray structural analyses and column chromatography, however, indicate that all of the crystals of the *R*-pn complexes consist of only the optically active isomers with Δ-*cis*(*S*)-[Co(aet)$_2$(*R*-pn)]$^+$ units to show negative CD signs around 500 nm in solution. Although two chiral configurations, *R* and *S*, are possible for each of the four bridging S atoms in all cases of **1**, **2**, and **3**, each of the S atoms is stereoselectively unified to the *R* configuration. It can therefore be concluded that the absolute configuration of the starting optically active complex, ΔΔ-[Ni{Co(aet)$_2$(*R*-pn)}$_2$]$^{4+}$, can be re-

Table 4. Selected Bond Distances (Å) and Angles (deg) of ΔΔ-$[Au_2\{Co(aet)_2(R\text{-pn})\}_2](ClO_4)_4\cdot H_2O$ (**3**$(ClO_4)_4\cdot H_2O$)

| | | | |
|---|---|---|---|
| Au(1)–Au(2) | 2.8775(7) | Au(1)–S(1) | 2.283(4) |
| Au(1)–S(3) | 2.299(4) | Au(2)–S(2) | 2.287(4) |
| Au(2)–S(4) | 2.280(4) | Co(1)–S(1) | 2.278(4) |
| Co(1)–S(2) | 2.250(4) | Co(1)–N(1) | 1.94(2) |
| Co(1)–N(2) | 2.00(1) | Co(1)–N(3) | 1.99(1) |
| Co(1)–N(4) | 2.01(1) | Co(2)–S(3) | 2.256(5) |
| Co(2)–S(4) | 2.256(4) | Co(2)–N(5) | 1.99(1) |
| Co(2)–N(6) | 1.98(1) | Co(2)–N(7) | 2.00(1) |
| Co(2)–N(8) | 1.98(1) | | |
| | | | |
| Au–(2)–Au(1)–S(1) | 94.07(10) | Au(2)–Au(1)–S(3) | 97.7(1) |
| S(1)–Au(1)–S(3) | 168.2(1) | Au(1)–Au(2)–S(2) | 98.08(10) |
| Au(1)–Au(2)–S(4) | 95.07(9) | S(2)–Au(2)–S(4) | 166.8(1) |
| S(1)–Co(1)–S(2) | 101.6(2) | S(1)–Co(1)–N(1) | 85.9(5) |
| S(1)–Co(1)–N(2) | 91.5(4) | S(1)–Co(1)–N(3) | 171.7(5) |
| S(1)–Co(1)–N(4) | 87.9(5) | S(2)–Co(1)–N(1) | 90.3(5) |
| S(2)–Co(1)–N(2) | 86.9(5) | S(2)–Co(1)–N(3) | 86.0(5) |
| S(2)–Co(1)–N(4) | 170.4(5) | N(1)–Co(1)–N(2) | 175.7(7) |
| N(1)–Co(1)–N(3) | 90.7(6) | N(1)–Co(1)–N(4) | 91.2(7) |
| N(2)–Co(1)–N(3) | 92.3(6) | N(2)–Co(1)–N(4) | 92.0(7) |
| N(3)–Co(1)–N(4) | 84.5(7) | S(3)–Co(2)–S(4) | 102.3(2) |
| S(3)–Co(2)–N(5) | 87.1(5) | S(3)–Co(2)–N(6) | 90.0(5) |
| S(3)–Co(2)–N(7) | 169.5(4) | S(3)–Co(2)–N(8) | 86.9(5) |
| S(4)–Co(2)–N(5) | 91.4(4) | S(4)–Co(2)–N(6) | 85.8(5) |
| S(4)–Co(2)–N(7) | 88.0(4) | S(4)–Co(2)–N(8) | 170.2(5) |
| N(5)–Co(2)–N(6) | 175.5(6) | N(5)–Co(2)–N(7) | 90.5(6) |
| N(5)–Co(2)–N(8) | 92.5(6) | N(6)–Co(2)–N(7) | 92.9(6) |
| N(6)–Co(2)–N(8) | 90.8(6) | N(7)–Co(2)–N(8) | 82.9(6) |
| Au(1)–S(1)–Co(1) | 119.8(2) | Au(2)–S(2)–Co(1) | 118.0(2) |
| Au(1)–S(3)–Co(2) | 118.2(2) | Au(2)–S(4)–Co(2) | 118.5(2) |

tained during the substitution reactions. In addition, all of the two aet and one *R*-pn chelate rings in each *cis*(*S*)-$[Co(aet)_2(R\text{-pn})]^+$ unit in **1**, **2**, and **3** take $\lambda$ conformations. These may be attributed to the fact that the methyl groups of the *R*-pn ligands take equatorial configurations.[27]

**Characterization.** As shown in Table 5, **1** exhibits seven $^{13}C$ NMR signals in a 1:1 mixed solvent of $CD_3CN$ and $D_2O$. Among these seven signals, the signals at 34.59 and 34.72 are due to the $-CH_2S$ groups, and the signals at 53.27 and 53.29 are due to the $-CH_2N$ groups in aet.[16,17] On the other hand, the signals at 17.68, 50.44, and 54.34 are assigned to the $-CH_3$, $-CH_2N$, and –CH groups in *R*-pn, respectively. These results imply that two *cis*(*S*)-$[Co(aet)_2(R\text{-pn})]^+$ units in **1** are almost equivalent to each other, and that the complex retains its symmetrical trinuclear structure in solution as in the solid state. **2** also shows only seven signals for fourteen carbon atoms of two *R*-pn and four aet ligands, indicating a symmetrical trinuclear structure in solution. While the $^{13}C$ NMR signals due to the $-CH_2S$ and $-CH_2N$ groups in aet are shifted toward downfield compared with the corresponding signals of **1**, those due to the $-CH_3$, $-CH_2N$, and –CH groups in *R*-pn are shifted toward upfield. This seems to reflect the differences of the central metal ions and their coordination modes. Similarly to the cases of **1** and **2**, **3** exhibits only seven $^{13}C$ NMR signals originated from the two equivalent *cis*(*S*)-$[Co(aet)_2(R\text{-pn})]^+$ units. Although the signals due to the $-CH_2S$ groups in aet appear at the downfield side compared with the corresponding signals of **1** and **2**, those due to the $-CH_2N$ groups in aet and the $-CH_3$ groups in *R*-pn appear at the upfield side. Furthermore, the signals due to the $-CH_2N$ and –CH groups in *R*-pn are located at the upfield side compared to the corresponding signals of **1**, but are located at the downfield side compared to those of **2**. These $^{13}C$ NMR spectral behaviors imply that the octahedral *cis*(*S*)-$[Co(aet)_2(R\text{-pn})]^+$ units in **1**, **2**, and **3** are situated at slightly different environments from each other. No other peaks were found in the spectra of **1**, **2**, and **3** for periods exceeding 1 week, indicating that these optically active S-bridged polynuclear structures are relatively stable in solution.

Table 5. $^{13}C$ NMR Chemical Shifts[a] of ΔΔ-$[Pt\{Co(aet)_2(R\text{-pn})\}_2]^{4+}$ (**1**), ΔΔ-$[Hg\{Co(aet)_2(R\text{-pn})\}_2]^{4+}$ (**2**), and ΔΔ-$[Au_2\{Co(aet)_2(R\text{-pn})\}_2]^{4+}$ (**3**)

| | **1** | **2** | **3** |
|---|---|---|---|
| $-CH_2S$ (aet) | 34.59 | 34.14 | 35.38 |
| | 34.72 | 34.27 | 35.48 |
| $-CH_2N$ (aet) | 53.27 | 53.14 | 52.16 |
| | 53.29 | 53.18 | 52.21 |
| –CHN (pn) | 54.34 | 55.31 | 55.27 |
| $-CH_2N$ (pn) | 50.44 | 51.42 | 51.21 |
| $-CH_3$ (pn) | 17.68 | 17.71 | 17.55 |

a) In ppm from TMS.

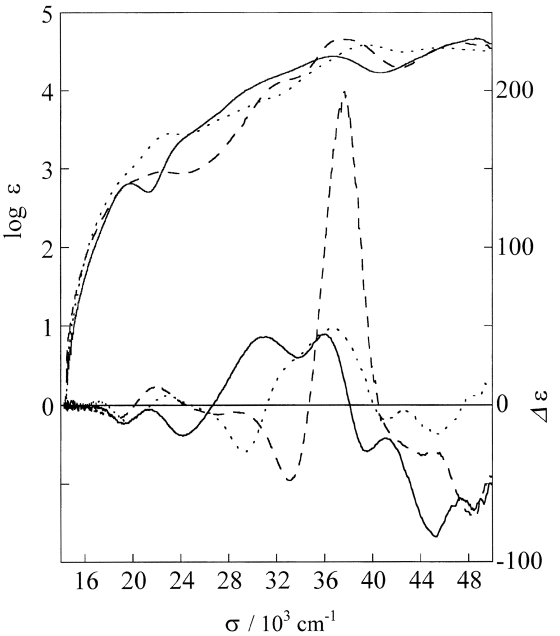


Fig. 4. Electronic absorption and CD spectra of ΔΔ-$[Pt\{Co(aet)_2(R\text{-pn})\}_2]^{4+}$ (**1**) (——), ΔΔ-$[Hg\{Co(aet)_2(R\text{-pn})\}_2]^{4+}$ (**2**) (– – –), and ΔΔ-$[Au_2\{Co(aet)_2(R\text{-pn})\}_2]^{4+}$ (**3**) (- - - - -) in $H_2O$.

The electronic absorption and CD spectra of **1**, **2**, and **3** in $H_2O$ are shown in Fig. 4, and their data are summarized in Table 6. The electronic absorption spectrum of **1** in $H_2O$ corresponds well with those of ΔΔ-$[Ni\{Co(aet)_2(R\text{-pn})\}_2]^{4+}$ and ΔΔ-$[Pd\{Co(aet)_2(R\text{-pn})\}_2]^{4+}$.[16,17] Namely, **1** shows two d–d bands due to the $Co^{3+}$ ion at 19.80 and 24.7 $\times$ $10^3$ $cm^{-1}$, one S-to-Co CT band at 36.76 $\times$ $10^3$ $cm^{-1}$, and three intense bands

Table 6. Electronic Absorption and CD Spectral Data of ΔΔ-$[Pt\{Co(aet)_2(R\text{-pn})\}_2]^{4+}$ (**1**), ΔΔ-$[Hg\{Co(aet)_2(R\text{-pn})\}_2]^{4+}$ (**2**), and ΔΔ-$[Au_2\{Co(aet)_2(R\text{-pn})\}_2]^{4+}$ (**3**)

| Absorption maxima $\sigma$ / $10^3$ cm$^{-1}$ (log $\varepsilon$ / mol$^{-1}$ dm$^3$ cm$^{-1}$) | | CD extrema $\sigma$ / $10^3$ cm$^{-1}$ ($\Delta\varepsilon$ / mol$^{-1}$ dm$^3$ cm$^{-1}$) | |
|---|---|---|---|
| ΔΔ-$[Pt\{Co(aet)_2(R\text{-pn})\}_2]^{4+}$ (**1**) | | | |
| 19.80 | (2.81) | 19.26 | (−12.18) |
| 24.7 | (3.4)$^{sh}$ | 24.18 | (−19.76) |
| 28.7 | (3.9)$^{sh}$ | 26.0 | (−8.2)$^{sh}$ |
| 30.4 | (4.1)$^{sh}$ | 31.13 | (+42.96) |
| 36.76 | (4.43) | 36.08 | (+44.38) |
| 48.54 | (4.66) | 39.62 | (−29.49) |
| | | 45.29 | (−84.24) |
| | | 48.45 | (−67.27) |
| ΔΔ-$[Hg\{Co(aet)_2(R\text{-pn})\}_2]^{4+}$ (**2**) | | | |
| 19.7 | (2.8)$^{sh}$ | 18.64 | (−8.08) |
| 22.40 | (2.95) | 21.83 | (+11.02) |
| 28.9 | (3.5)$^{sh}$ | 27.06 | (−6.47) |
| 32.0 | (4.1)$^{sh}$ | 33.11 | (−48.23) |
| 37.59 | (4.65) | 36.5 | (+139.6)$^{sh}$ |
| 38.8 | (4.6)$^{sh}$ | 37.71 | (+199.18) |
| 47.39 | (4.62) | 42.1 | (−22.7)$^{sh}$ |
| | | 44.09 | (−32.41) |
| | | 48.54 | (−72.00) |
| ΔΔ-$[Au_2\{Co(aet)_2(R\text{-pn})\}_2]^{4+}$ (**3**) | | | |
| 19.4 | (2.9)$^{sh}$ | 19.83 | (−10.50) |
| 23.18 | (3.44) | 22.79 | (+5.55) |
| 27.0 | (3.6)$^{sh}$ | 25.8 | (−3.1)$^{sh}$ |
| 30.6 | (3.8)$^{sh}$ | 29.31 | (−30.06) |
| 35.0 | (4.2)$^{sh}$ | 33.0 | (+24.8)$^{sh}$ |
| 39.53 | (4.58) | 36.60 | (+48.56) |
| 45.7 | (4.5)$^{sh}$ | 41.12 | (−9.98) |
| | | 45.29 | (−19.21) |
| | | 47.2 | (−5.9)$^{sh}$ |

The sh label denotes a shoulder.

related to the $Pt^{2+}$ ion at 28.7, 30.4, and 48.54 × $10^3$ cm$^{-1}$. While the partial structures of the *cis*(*S*)-$[Co(aet)_2(R\text{-pn})]^+$ units in the Ni(II), Pd(II), and Pt(II) complexes are almost identical to each other, the energies for the transition concerning $Co^{3+}$ ions are slightly different from each other. This implies that the distinctions of the central metal ions in the trinuclear structures electronically influence the terminal Co(III) units. On the other hand, the CD spectral pattern of **1** is similar to those of ΔΔ-$[Ni\{Co(aet)_2(R\text{-pn})\}_2]^{4+}$ and ΔΔ-$[Pd\{Co(aet)_2(R\text{-pn})\}_2]^{4+}$ over the whole region. For instance, the CD spectral signs in the first d-d absorption regions, which are sensitive for the structures of the octahedral Co(III) units,[28] are of the same as each other. This supports the consistency in the absolute configurations of the two terminal Co(III) units between the three complexes. Reflecting two Δ-*cis*(*S*)-$[Co(aet)_2(R\text{-pn})]^+$ units in the S-bridged polynuclear structures, both of **2** and **3** show a similar absorption and CD spectral trends to **1**. As would be predicted by the crystal structures of **1**, **2**, and **3**, however, the transitions related on the $Co^{3+}$ ions are influenced by the differences in the bond distances and angles around the Co(III) atoms. Thus, the d–d and S-to-Co CT bands for these complexes are located at slightly distinct positions. Each of the complexes shows two intense CD bands with positive signs in the region of 24 – 44 × $10^3$ cm$^{-1}$, i. e., the positive bands at 31.13 and 36.08 × $10^3$ cm$^{-1}$ for **1**, 36.5 and 37.71 × $10^3$ cm$^{-1}$ for **2**, and 33.0 and 36.60 × $10^3$ cm$^{-1}$ for **3**. Among these bands, the higher energy side one in each complex is accompanied by a negative CD component at the higher-energy side (39.62 × $10^3$ cm$^{-1}$ for **1**, 42.1 × $10^3$ cm$^{-1}$ for **2**, and 41.12 × $10^3$ cm$^{-1}$ for **3**), and assigned as an S-to-Co CT transition.[16,17] On the other hand, the lower energy side band in each complex is accompanied by a negative CD component at the lower energy side (26.0 × $10^3$ cm$^{-1}$ for **1**, 33.11 × $10^3$ cm$^{-1}$ for **2**, and 29.31 × $10^3$ cm$^{-1}$ for **3**). It is noteworthy that the extent of the splitting between the two positive bands is significantly different from each other. Especially for **2**, the two positive bands (36.5 and 37.71 × $10^3$ cm$^{-1}$) are split only by 1.2 × $10^3$ cm$^{-1}$, in contrast to the cases of **1** (3.54 × $10^3$ cm$^{-1}$) and **3** (3.6 × $10^3$ cm$^{-1}$). Since the higher energy side band due to S-to-Co CT transitions is less shifted than the lower energy side band, the lower energy side band can be regarded as being sensitive for the incorporated metal ions, and is assigned as S-to-M (M = $Pt^{II}$, $Hg^{II}$, $Au^{I}$) or M-to-S CT transition. It can therefore be concluded that the absorption and CD spectral behaviors of such S-bridged Co$^{III}$M polynuclear complexes are largely dependent on the incorporated metal ions as well as the structures of the terminal octahedral Co(III) units.

This work was partially supported by Grants-in-Aid for Scientific Research Nos. 11640555 and 12023205 from the Ministry of Education, Science, Sports, and Culture.

## References

1 D. C. Jicha and D. H. Busch, *Inorg. Chem.*, **1**, 872 (1962).
2 D. C. Jicha and D. H. Busch, *Inorg. Chem.*, **1**, 878 (1962).
3 C. H. Wei and L. F. Dahl, *Inorg. Chem.*, **9**, 1878 (1970).
4 K. Okamoto, C. Sasaki, Y. Yamada, and T. Konno, *Bull. Chem. Soc. Jpn.*, **72**, 1685 (1999), and references therein.
5 Y. Miyashita, Y. Yamada, K. Fujisawa, T. Konno, K. Kanamori, and K. Okamoto, *J. Chem. Soc., Dalton Trans.*, **2000**, 981.
6 Y. Yamada, M. Uchida, Y. Miyashita, K. Fujisawa, T. Konno, and K. Okamoto, *Bull. Chem. Soc. Jpn.*, **73**, 913 (2000).
7 Y. Yamada, K. Fujisawa, and K. Okamoto, *Bull. Chem. Soc. Jpn.*, **73**, 2067 (2000).
8 Y. Yamada, K. Fujisawa, and K. Okamoto, *Bull. Chem. Soc. Jpn.*, **73**, 2297 (2000).
9 T. Konno, K. Tokuda, J. Sakurai, and K. Okamoto, *Bull. Chem. Soc. Jpn.*, **73**, 2767 (2000).
10 T. Konno, M. Hattori, T. Yoshimura, and M. Hirotsu, *Chem. Lett.*, **2000**, 852.
11 T. Konno, K. Tokuda, K. Okamoto, and M. Hirotsu, *Chem. Lett.*, **2000**, 1258.
12 Y. Yamada, Y. Miyashita, K. Fujisawa, and K. Okamoto, *Bull. Chem. Soc. Jpn.*, **74**, 97 (2001).
13 T. Konno, Y. Chikamoto, K. Okamoto, T. Yamaguchi, T. Ito, and M. Hirotsu, *Angew. Chem., Int. Ed.*, **39**, 4098 (2001).
14 Y. Miyashita, M. Hamajima, Y. Yamada, K. Fujisawa, and K. Okamoto, *J. Chem. Soc., Dalton Trans.*, **2001**, 2089.
15 Y. Miyashita, N. Mahboob, S. Tsuboi, Y. Yamada, K. Fujisawa, and K. Okamoto, *Bull. Chem. Soc. Jpn.*, **74**, 1295

(2001).

16 Y. Yamada, Y. Maeda, Y. Miyashita, K. Fujisawa, T. Konno, and K. Okamoto, *Bull. Chem. Soc. Jpn.*, **73**, 1219 (2000).

17 Y. Yamada, Y. Maeda, T. Konno, K. Fujisawa, and K. Okamoto, *Bull. Chem. Soc. Jpn.*, **73**, 1831 (2000).

18 H. D. Flack, *Acta Crystallogr., Sect. A*, **39**, 876 (1983).

19 H. D. Flack and G. Bernandinello, *Acta Crystallogr., Sect. A*, **41**, 500 (1985).

20 "teXsan. Molecular Structure Corporation. Single Crystal Structure Analysis Software. Version 1.9," MSC, 3200 Research Forest Drive, The Woodlands, TX77381, USA (1998).

21 Lists of final atomic coordinates and equivalent isotropic thermal parameters for hydrogen atoms, anisotropic thermal parameters for non-hydrogen atoms, and bond distances and angles are deposited as Document No. 75023 at the Office of the Editor of Bull. Chem. Soc. Jpn.

22 E. C. Constable, *Coord. Chem. Rev.*, **62**, 27 (1985).

23 E. S. Gruff and S. A. Koch, *J. Am. Chem. Soc.*, **112**, 1245 (1990).

24 C. Lensch, P. G. Jones, and G. M. Sheldrick, *Z. Naturforsch, Teil B*, **37**, 944 (1982).

25 S. Hofreiter, M. Paul, and H. Schmidbaur, *Chem. Ber.*, **128**, 901 (1995).

26 F. Canales, M. C. Gimeno, A. Laguna, and P. G. Jones, *J. Am. Chem. Soc.*, **118**, 4839 (1996).

27 E. J. Corey and J. C. Bailar, Jr., *J. Am. Chem. Soc.*, **81**, 2620 (1959).

28 C. J. Hawkins, "Absolute Configurations of Metal Complexes," Wiley-Interscience, New York (1971).